Structure of Lamellar Lipid Domains and Corneocyte Envelopes of Murine Stratum Corneum. An X-ray Diffraction Study†

Stephen H. White,*,‡ Dorla Mirejovsky,§ and Glen I. King‡,∥

Department of Physiology and Biophysics, University of California, Irvine, Irvine, California 92717, and Allergan, Inc., Irvine, California 92715

Received September 1, 1987; Revised Manuscript Received January 12, 1988

ABSTRACT: The lipid of the outermost layer of the skin is confined largely to the extracellular spaces surrounding the corneocytes of the stratum corneum where it forms a multilamellar adhesive matrix to act as the major permeability barrier of the skin. Knowledge of the molecular architecture of these intercellular domains is important for understanding various skin pathologies and their treatment, percutaneous drug delivery, and the cosmetic maintenance of the skin. We have surveyed by X-ray diffraction the structure of the intercellular domains and the extracted lipids of murine stratum corneum (SC) at 25, 45, and 70 °C which are temperatures in the vicinity of known thermal phase transitions [Rehfeld, S. J., & Elias, P. M. (1982) *J. Invest. Dermatol. 79*, 1–3]. The intercellular domains produce lamellar diffraction patterns with a Bragg spacing of 131 ± 2 Å. Lipid extracted from the SC and dispersed in excess water does not produce a simple lamellar diffraction pattern at any temperature studied, however. This and other facts suggest that another component, probably a protein, must be present to control the architecture of the intercellular lipid domains. We have also obtained diffraction patterns attributable to the protein envelopes of the corneocytes. The patterns suggest a β-pleated sheet organizational scheme. No diffraction patterns were observed that could be attributed to keratin.

The sole permeability barrier of the external surfaces of terrestrial vertebrates is the stratum corneum (SC)[1] which constitutes the outermost layer of the epidermis (Marks & Plewig, 1983; Schaefer et al., 1982). As shown schematically in Figure 1, the SC consists of corneocytes filled with keratin filaments surrounded by a tough protein envelope running along the inner surface of the plasma membrane (Brody, 1959; Farbman, 1966). The intercellular spaces between the corneocytes are filled with apparently lamellar sheets of lipid, as determined by EM, which act in part as an adhesive matrix surrounding the corneocytes (Elias & Friend, 1975; Lavker, 1976; Elias et al., 1977; Hayward, 1978; Landmann, 1980, 1986). This lipid matrix is believed to be the major pathway by which water and other substances traverse the SC (Blank, 1952; Elias & Friend, 1975; Elias et al., 1977, 1981; Smith et al., 1982; Elias, 1983; Golden et al., 1987). Information about the molecular organization of this region is important for understanding diseases of the SC (Elias, 1983) and for the rational design of chemical modifiers used to enhance the delivery of drugs percutaneously (Woodford & Barry, 1986).

X-ray diffraction is the ideal method for studying the lipid domains because of its general usefulness for revealing the structure and organization of assemblies of biological lipids [see, e.g., Franks and Levine (1981) and Small (1986)]. Surprisingly, there have been only a few X-ray diffraction studies of SC and its lipids. The earliest studies suggested that the lipid formed a lamellar sheath around the keratin filaments (Swanbeck, 1959; Swanbeck & Thyresson, 1961, 1962; Goldsmith & Baden, 1970; Wiles et al., 1973) but a later wide-angle study supported the notion of the lipid being in the intercellular spaces (Elias et al., 1983). Friberg et al. (1985) reported small-angle X-ray measurements on human SC in the context of skin softeners, but the patterns presented were broad and largely featureless. Taken together, these studies provide a rather meager view of the lipid organization of the SC. None of them demonstrated directly or convincingly the presence of lamellar intercellular lipid domains, and it was thus not certain at the outset that the experiments described below would be fruitful.

The work we describe represents a broad survey of the general X-ray diffraction features of the SC carried out for the purpose of establishing the feasibility and potential usefulness of more detailed diffraction studies. We wished to answer three questions. First, can diffraction patterns be obtained which are attributable to the lipid domains? Second, is there a simple relationship between the organization of the lipids in situ and of the extracted lipids in vitro? Third, are there other structural features present which might be attributable to nonlipid components such as keratin?

We chose to perform our diffraction studies on the SC of hairless mice because this preparation is in common use for percutaneous drug delivery studies (Mirejovsky & Takruri, 1986). The lipid composition of the SC of the strain of mice we used is typical of that observed among a number of mammalian species (Elias et al., 1979; Bowser & White, 1985; Lampe et al., 1983). There is about 52% neutral lipid (sterols, triglycerides, sterol esters, and alkanes), 36% ceramides, 11% free fatty acids, and 1% cholesterol sulfate (D. Mirejovsky and G. F. Ambrus, unpublished results). The predominant acyl chains are C16:0, C18:1, and C24:0. The SC is unusual for the near absence of phospholipids normally associated with lamellar membrane systems; the ceramides are the dominant

† Supported by a gift from Allergan, Inc., and in part by grants from the National Science Foundation (DMB-8412754) and the National Institutes of Health (GM-37291).

* Correspondence should be addressed to this author.
‡ University of California, Irvine.
§ Allergan, Inc.
∥ Present address: 320 Loyola Dr., Aptos, CA 94704.

[1] Abbreviations: SC, stratum corneum; EM, electron microscopy; MCG, membrane-coating granule(s).

0006-2960/88/0427-3725$01.50/0

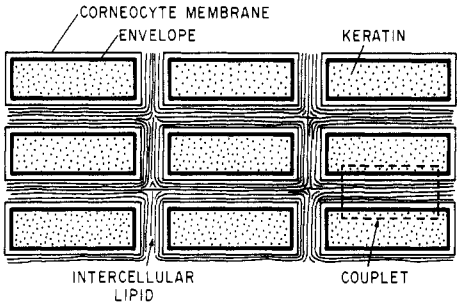

FIGURE 1: Schematic representation of the organization of the stratum corneum (SC). The SC is the outermost layer of the epidermis and is the sole permeability barrier of the external surfaces of terrestrial vertebrates. The lipid matrix surrounding the corneocytes is believed to be the major pathway by which water and other substances traverse the SC.

species. The only other tissue which contains ceramides in abundance is the nervous system which, interestingly, shares the skin's embryonic origins.

Calorimetric and IR spectroscopic studies suggest that the lipids of the intact mouse SC undergo thermal phase transitions at about 35 and 65 °C (Rehfeld & Elias, 1982; Knutson et al., 1985). One of the secondary goals of our study was to obtain direct structural information on the organization of the intercellular lipids in the vicinity of these phase transitions. To do this, we performed X-ray diffraction measurements at 25, 45, and 70 °C on whole SC, on the lipids extracted from the SC, on isolated envelope–lipid complexes ("couplets"; see Figure 1) (Grayson & Elias, 1982), and on lipid-extracted couplets. Because the amounts of lipid available to us were limited and because the study was a general survey, we decided to examine at a later time the effects of water and electrolyte activities. All measurements were thus made at constant water activity; samples were prepared only in excess distilled water.

We demonstrate here the direct X-ray diffraction observation of the lamellar organization of the intercellular lipid domains in situ and show that the organization of the lipid is different in vitro. Further, we have obtained X-ray diffraction patterns attributable to the protein envelopes of the corneocytes. The patterns suggest a β-pleated sheet organizational scheme. We did not observe any diffraction patterns attributable to keratin.

Materials and Methods

Preparation of Stratum Corneum Samples. Stratum corneum sheets were isolated by a modification of the method of Lampe et al. (1983) from the dorsal skins of 6–9-week-old male mice (strain: Allergan SKH-hairless-1). The second trypsinization was eliminated from the Lampe et al. procedure; complete removal of the granulosum layer was confirmed by light microscopy. Samples for diffraction were generally prepared by packing small SC fragments into 1-mm X-ray capillaries. Some experiments were also performed on SC which had been oriented by wrapping it tightly around a 0.5-mm capillary prior to insertion into the 1-mm capillary. In all cases, the capillaries contained a small amount of excess water.

Preparation of Stratum Corneum Couplets. Couplets were graciously prepared for us by Dr. Stephen Grayson using the method of Grayson and Elias (1982). In brief, the isolated SC sheets are frozen in liquid N_2, pulverized with a cold hammer, suspended in buffer, and homogenized by passage at 20000–30000 psi through a Stansted cell disrupter (Stansted Fluid Power Corp. Ltd., Stansted, Essex, U.K.). After centrifugation of the homogenate, the resuspended pellet is digested with subtilisin (protease VIII, Sigma) which removes virtually all of the keratin without affecting the corneocyte envelope or intercellular lipids. The absence of keratin filaments was confirmed by EM.

Lipid Extraction and Sample Preparation. Lipid was extracted by the method of Bligh and Dyer (1959) using the skins of approximately 150 mice which produce about 1 mg of lipid each. Lipids from the aqueous and organic phases were pooled together. Samples were prepared for diffraction by heating the lipid and excess water to 85 °C and mixing thoroughly followed by several additional heating–mixing–cooling cycles. The samples were then placed in capillaries and then into the X-ray camera's thermostat where they were heated to 70 °C and allowed to anneal for several hours. Patterns from lipids at 45 and 25 °C were obtained from samples cooled slowly (3 h) from 70 °C.

X-ray Diffraction. All patterns shown in this paper were recorded on Kodak DEF-5 film using a helium-filled Elliott (1965) toroidal camera with D-sector optics. X-rays were produced by a Jarrell–Ash generator with Cu anode (38 kV, 6.5 mA) and a nickel filter to isolate Kα radiation (λ = 1.542 Å). The film to sample distance (d_{fs}) was determined by using a National Bureau of Standards d-spacing standard (NBS 675, d = 9.981 Å). The exposure times used were generally 6–8 h for the lipid samples and 12–24 h for the SC samples.

The toroidal camera was chosen for this study because of the intense well-focused beam it is capable of producing. This turned out to be the most essential requirement for the experiments on the SC tissue because of the relatively low intensity of the generators available to us and because the intercellular lipid domains represent a very small fraction (5% or less) of the total sample in the beam. Good diffraction patterns could not be obtained with exposures of much less than 12 h; 18–24-h exposures were generally best. The major deficiency of the toroidal camera is that it cannot reveal spacings greater than ~100 Å. This limitation precluded a detailed structural analysis of the intercellular lipid domains which have a Bragg spacing of ~130 Å. Only diffraction orders with $h \geq 2$ could be observed reliably. We thus tried experiments with a camera with double-mirror optics capable of resolving spacings of 1000 Å (Franks, 1958). Unfortunately, such cameras reduce the intensity of the beam by about 10-fold relative to the toroid and would thus require exposure times of 120–240 h. However, some very much shorter exposures were made with the Franks camera to at least confirm the existence of the first-order lamellar diffraction line of the intercellular domains. The patterns were too weak to provide useful quantitative intensity data.

Model Calculations. The relative intensities and phases of the diffraction peaks from the lamellar intercellular lipid domains permit one to calculate the electron density profiles of the unit cell of the domains. In the present study, however, the intensity of the first-order peak could not be determined accurately, and no experiments were performed to establish the phases of the peaks. Nevertheless, some useful information about the unit cell can be obtained from intensities alone as demonstrated by Worthington and Blaurock (1969) for nerve myelin. In particular, we use their approach to examine the consequences of the symmetry properties of unit cells containing two bilayers, protein, and water. The basic procedure is to construct electron density versus distance strip models of possible arrangements of the bilayers, protein, and water. The widths of the strips are chosen to be consistent with the resolution of the experiment and the heights of the strips chosen to represent the average electron density of the region

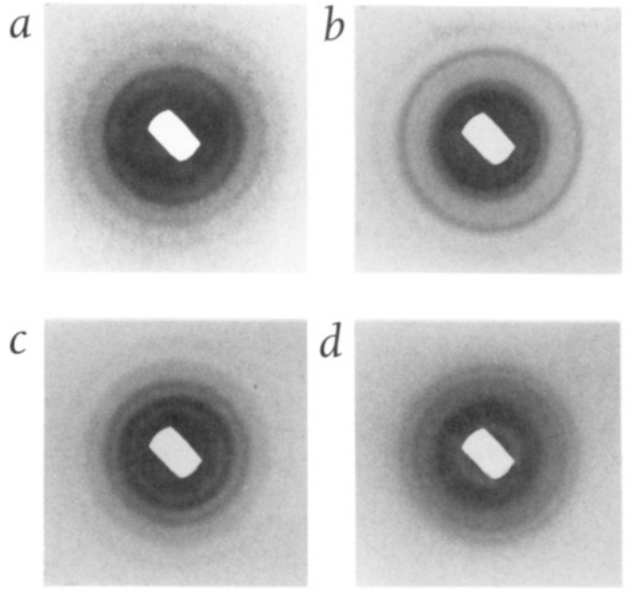

FIGURE 2: Small-angle diffraction patterns from intact hairless mouse stratum corneum (SC) at 25 °C (a) and from extracted lipids at 25 (b), 45 (c), and 70 °C (d). Excess water is present in all cases. Four orders (h = 2, 3, 4, 5) of lamellar diffraction with d_1 = 131 ± 2 Å are observed in the intact SC pattern shown in (a). The lipid extracted from the SC gives nonlamellar patterns (b–d) at all temperatures examined. The patterns in (b), (c), and (d) index respectively as an oblique lattice, a rectangular lattice, and a hexagonal lattice (see text for lattice parameters). The film to sample distance (d_{fs}) in (a) was 8.15 cm and in (b–d) 6.93 cm. The width of the beam stopper is 0.13 cm.

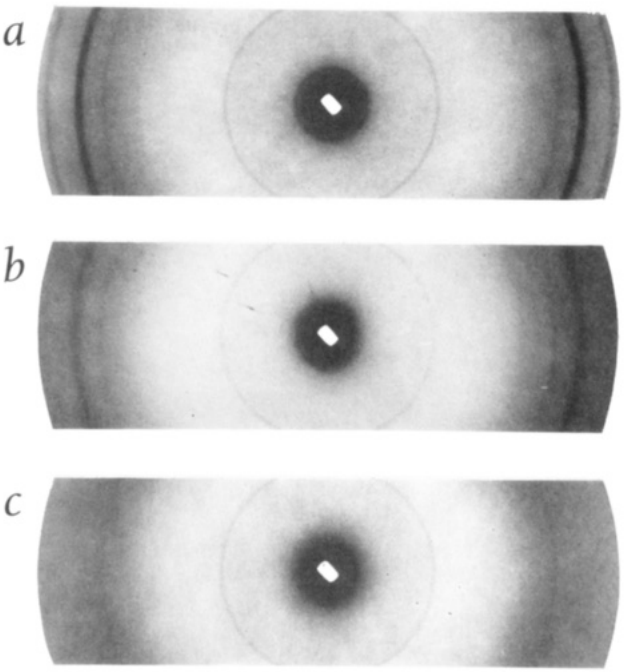

FIGURE 3: Diffraction patterns of intact SC at 25 (a), 45 (b), and 70 °C (c). The wide-angle lines assigned to lipid alkyl chain packing in Figure 4 are also seen here. In addition, two new lines are observed at 4.6 and 9.4 Å which are unaffected by temperature. These lines originate from the protein in the envelope of the corneocytes (see Figure 5 and text). The lack of well-defined keratin scattering of the type reported by Swanbeck (1959) for human thick SC should be noted. Interesting changes with temperature are also observed in the small-angle regions of these patterns (see text). d_{fs} = 6.94 cm.

of the unit cell defined by the width. Fourier transformation of the electron densities yields test values of structure factors. The squares of the structure factors provide estimates of the relative intensities of the diffraction lines. The procedures and equations for such calculations have been described in detail by King and White (1986).

Results

Small-Angle Diffraction from Intact SC. The small-angle diffraction pattern of oriented intact SC obtained with the toroidal camera at 25 °C shows four orders (h = 2, 3, 4, 5) of lamellar diffraction with a repeat period (Bragg spacing) of 131 ± 2 Å (Figure 2a). A few experiments were performed using a Franks (1958) camera with double-mirror optics (see Materials and Methods). The resulting very weak patterns showed three orders (h = 1, 2, 3) of lamellar diffraction with a repeat period of 132 Å (data not shown). None of the patterns revealed a preferred orientation which is consistent with the naturally rippled configuration of the SC and the fact that the lipid domains cover all surfaces of the corneocytes. The observed lines in Figure 2a are very sharp, indicating that the diffraction originates from an ordered lattice with many unit cells.

Significant reversible changes are observed in the small-angle (lamellar) pattern of the intact SC as the temperature is increased (data not shown). The pattern becomes very diffuse at 45 °C and "smoky" in appearance; there are hints of structure but nothing more. At 70 °C, the pattern is that expected of an amorphous substance. There seems to be a major disorganization of the lipid domains as the temperature is increased. Returning the intact SC to 25 °C after several days at the elevated temperatures completely restores the lamellar pattern with practically no change in d spacing.

Wide-Angle Diffraction from Intact SC. The wide-angle diffraction patterns obtained at 25, 45, and 70 °C (Figure 3) are consistent with the phase transitions of SC observed by Rehfeld and Elias (1982). The common features among the patterns which are unaffected by temperature are sharp lines at 9.4 and 4.6 Å which we attribute to the corneocyte envelopes (vida ut infra). The other lines we attribute to diffraction from the lipid alkyl chains because similar ones are observed in extracted lipids (vide ut infra). At 25 °C (Figure 3a), there are two sharp lines at 3.75 and 4.16 Å and a broad diffuse one at about 4.6 Å. We interpret this to mean that crystalline and liquid alkyl chains coexist in the structures. At 45 °C (Figure 3b), the two sharp lines are replaced by a single one at 4.12 Å which we interpret as a transition from a crystalline to a gel state in which alkyl chains are free to rotate about their axes. This suggests either a major packing change ("melting") of all the lipids or the selective melting of certain lipids. (The rather broad 4.16-Å line seen at 25 °C may be obscuring the 4.12-Å line so that both crystalline- and gel-state alkyl chains may be present at 25 °C.) At 70 °C (Figure 3c), none of the lipid is in a gel or crystalline state, and only the broad 4.6-Å line characteristic of liquid hydrocarbons is seen. We note that Wilkes et al. (1973) observed at 25 °C two sharp wide-angle lines from neonatal rat SC at 3.7 and 4.2 Å; the 3.7-Å line was absent at 40 °C and the 4.2-Å line at 70 °C. Goldsmith and Baden (1970) reported a line at 4.15 Å from "mammalian" SC attributed to lipid. Elias et al. (1983) found lines at 3.75 and 4.16 Å from whole mouse SC and SC couplets. (Whole lipid extracts showed 17 lines ranging from 1.3 to 10.8 Å, but the hydration state was not specified; we suspect the lipid had a very small water content and was in a crystalline form.)

Diffraction from Lipid Extracts. Simple lamellar diffraction patterns were never observed in the lipid extracts at any temperature as shown in Figure 2b–d. The extracts are a complex mixture of lipids, and one might expect several phases to be present simultaneously. The simplest possibility would be two or more lamellar phases. However, attempts

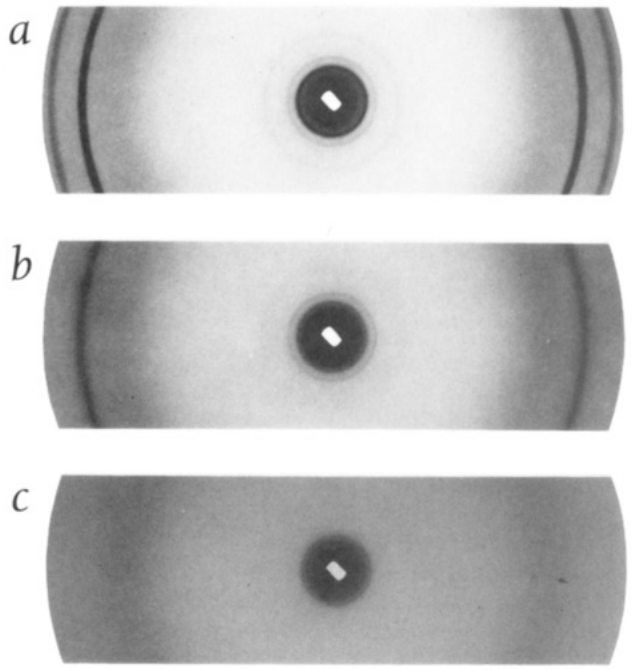

FIGURE 4: Wide-angle diffraction patterns from total lipid extracts in excess water at 25 (a), 45 (b), and 70 °C (c). The patterns are from the same films as in Figure 2b–d. A diffuse band at 4.5–4.6 Å is observed at all temperatures, indicating the presence of melted lipid alkyl chains. In (a), two additional sharp lines at 3.75 and 4.16 Å are observed, indicating crystalline lipids. They likely arise from an orthorhombic perpendicular subcell of crystalline alkyl chains. In (b), these two lines are replaced by a single somewhat less sharp line at 4.12 Å due to gel-state alkyl chains; in this case, the alkyl chain subcell is hexagonal. In (c), all of the lipid appears to be in the liquid state.

to index the patterns at 25 and 45 °C assuming this to be the case failed, and we therefore sought two-dimensional lattices. The pattern obtained at 25 °C (Figure 2b) could be indexed as a two-dimensional oblique lattice with lattice constants a = 59 Å, b = 90.5 Å, and γ = 98°. At 45 °C (Figure 2c), the pattern indexes as rectangular with a = 47 Å and b = 150 Å and at 70 °C (Figure 2d) as a hexagonal lattice with a = 67 Å. These lattice assignments must, however, be considered as tentative until additional experiments are performed at lower hydrations. While we do not yet have enough data to determine the structures of the hydrated lipid assemblies at the different temperatures, it is clear that changes in lipid organization do occur at approximately the temperatures expected from the calorimetric studies on whole mouse SC.

Unlike the small-angle patterns, the wide-angle patterns of the lipid extracts (Figure 4) corresponded exactly at each temperature with the patterns from intact SC (Figure 3) except for the sharp lines at 9.4 and 4.6 Å (vide ut infra). We take this to mean that the lateral packing of the lipids in situ and in vitro is the same.

Diffraction Patterns from Isolated Envelope–Lipid Complexes. The data of Figure 2–4 are generally consistent with the hypothesis that the SC lamellar diffraction pattern arises from lipid in the interstitial spaces. As a further test of the hypothesis, we examined corneocyte membrane/intercellular lipid couplets. The wide-angle diffraction pattern (Figure 5a) from these couplets is virtually identical with that of the intact SC (Figure 3a). Extensive lipid extraction of the couplets completely removed the components of the diffraction pattern attributable to the lipid as shown in Figure 5b. Note, however, that the lines at 9.4 and 4.6 Å remain. Further, on the original films, another line becomes visible at 3.9 Å after lipid extraction.

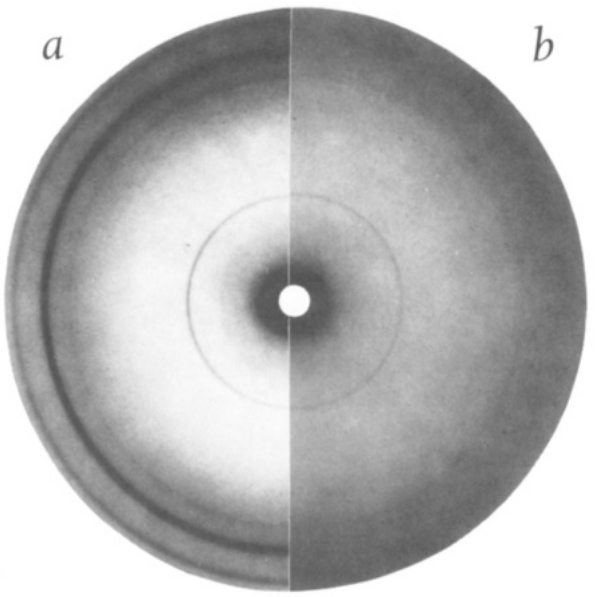

FIGURE 5: Diffraction patterns of isolated SC couplets (a) and of couplets extracted of lipid (b) at 25 °C. SC couplets, isolated by the method of Grayson and Elias (1982), consist generally of adherent pairs of corneocyte cell envelopes separated by the intercellular lipid (Figure 1). The couplets are devoid of keratin filaments. The wide-angle pattern of the couplets in (a) is nearly indistinguishable from that of the intact SC seen in Figure 3a. The small-angle spacings of the couplets have a different form; they appear to be mostly continuous diffraction with an admixture of a small amount of discrete diffraction (see text). Peaks appear at 126, 63, 32, and 23 Å. The diffraction pattern of the lipid-extracted couplets in (b) lacks the wide-angle lines characteristic of the SC lipid. Further, the small-angle pattern becomes completely amorphous. Both (a) and (b) retain the sharp lines at 4.6 and 9.4 Å but the 4.6-Å line is somewhat weakened. In (b), a weak line at about 3.9 Å is visible on the original film. Because the corneocyte envelopes are the only structures remaining after lipid extraction, these lines must arise from the envelopes (see text). d_{fs} = 6.93 cm.

The small-angle diffraction pattern of the couplets is different from that of the intact SC (data not shown). There is a clear pattern, but it consists of what appears to be continuous diffraction with a small admixture of discrete diffraction. The location of the first maximum corresponds to a spacing of about 126 Å. This pattern is completely destroyed by lipid extraction which causes it to change to pure amorphous scattering.

Discussion

Organization of the Intercellular Domains. One of our primary goals was to demonstrate that diffraction patterns can be obtained directly from the intercellular lipid domains of intact stratum corneum. The accomplishment of this goal is supported by the fact that equivalent wide-angle diffraction patterns are observed in intact SC, SC couplets, and extracted lipids. In addition, the patterns change in characteristic and equivalent ways with temperature, and the changes are clearly correlated with the thermal phase transitions of intact SC observed by Rehfeld and Elias (1982). Furthermore, extraction of the lipids from the SC couplets completely abolishes the wide-angle diffraction lines attributable to the lipids. These results are consistent with electron microscopic observations of multilamellar intercellular domains in intact SC and couplets which are abolished by lipid extraction (Grayson & Elias, 1982). The fact that the wide-angle patterns are observed in the keratin-free couplets rules out the possibility of the lipid being closely associated with the keratin filaments as proposed by Swanbeck (1959). There can be little doubt that diffraction

patterns can be obtained directly from the intercellular domains.

Given the equivalence of the high-angle diffraction patterns from intact SC, SC couplets, and extracted lipids, one can also reasonably conclude that the lateral packing of the lipids is equivalent in all three systems. The wide-angle patterns indicate that both liquid and "solidified" alkyl chains are present at 25 and 45 °C. At 70 °C, only a broad 4.5–4.6-Å band is present, indicating that all hydrocarbon chains are in the liquid state. This broad band persists at all temperatures, but additional sharp lines are seen at 25 and 45 °C. The 3.75- and 4.16-Å lines seen at 25 °C are characteristic of crystalline alkyl chains organized as an orthorhombic perpendicular subcell. [See Small (1986) for a thorough discussion of alkyl chain subcells.] At 45 °C, these lines are replaced by a single less sharp line at 4.12 Å which is that expected of gel-state alkyl chains organized as ordered hexagonal subcells. The alkyl chains are free to undergo axial rotations in the gel state. Because of the width of the 4.16-Å line, we cannot rule of the possibility of a population of alkyl chains in the gel state at 25 °C as well.

A particularly interesting observation is the nonequivalence of the small-angle diffraction patterns observed in extracted lipids, intact SC, and couplets. Given the simple lamellar diffraction patterns obtained from intact SC, it was somewhat surprising that the small-angle patterns obtained from the lipid extracts in excess water were never those which are usually seen in single or multiple lipid phases composed of simple multilamellar structures. All attempts to index the patterns as lamellar structures or mixtures of lamellar structures failed. While there is not yet enough information to be compeltely certain of the lattice structures, the observed patterns fit quite well oblique, rectangular, and hexagonal lattices at 25, 45, and 70 °C, respectively. The simultaneous existence of gel and liquid alkyl chains at 25 and 45 °C and the apparent organization of the lipids as two-dimensional lattices suggest that the lipids may be organized as rippled or peristaltic bilayer lamellae. Such organizational schemes have been seen in other complex lipid mixtures and arise in part from the coexistence of liquid- and gel-state acyl chains in the same lamellae (Ranck et al., 1974). If this is the situation for the extracted SC lipids, then it is reasonable to attribute the repeat distance of the lamellae to the lattice parameters a = 59 and 47 Å at 25 and 45 °C, respectively. The lattice parameters b = 90.5 and 150 Å would characterize the in-plane repeat distance of the lamellae due to the putative ripples. This type of structure is seen most clearly perhaps in the $P_{\beta'}$ phase of dimyristoyllecithin (Janiak et al., 1979). There one observes rippled lamellae with values of a = 55.9–59.6 Å and b = 160.9–118 Å depending upon hydration.

While some doubt must remain about the precise structure of the lipid phases at 25 and 45 °C pending further experiments, there is less doubt about the situation at 70 °C. The small-angle pattern clearly indexes as hexagonal, and all of the alkyl chains are in the liquid state. The lipids very likely form a hexagonal II phase (lattice parameter 67 Å) consisting of polar head-group-lined tubes filled with water stacked lengthwise in piles on a hexagonal lattice [see Small (1986)]. Hexagonal I phase (alkyl chain-filled tubes) can be ruled out because it cannot coexist with an excess water phase. It is of interest in this regard that Golden et al. (1987) have observed large increases in the water permeability of porcine SC accompanied by large decreases in activation energy above 70 °C, there are phase transitions in this tissue at 65 and 70 °C.

The small-angle diffraction pattern obtained from intact SC is strikingly different from those obtained from the extracted lipids (Figure 2) in two respects. First, at 25 °C, the pattern is that expected of a lamellar structure containing many unit cells in a highly ordered lattice with a repeat distance of 131 ± 2 Å. The most likely repeat distance of the possibly rippled lamellae of the extracted lipids is about 60 Å. Second, the diffraction patterns become progressively disordered as the temperature is increased, culminating in apparently amorphous scattering at 70 °C. There are no signs of well-defined changes in phase as observed for the extracted lipids. Significantly, when samples are cooled back to 25 °C, the lamellar pattern returns with a Bragg spacing which is the same as the preheating value. This suggests that another component(s) is (are) present in the intercellular space which helps maintain(s) the lamellar organization. We rather expected from the amorphous scattering at high temperatures that the intercellular domains were being irreversibly disrupted. In such a case, one might have expected that after prolonged heating the diffraction patterns would have eventually resembled those of the extracted lipids. The supposed "second component" would have to have a rather tight structural relationship with the lipids which would permit restoration of the lamellar phase at low temperatures but prevent the appearance of a hexagonal phase at high temperatures. It is thus particularly interesting that the wide-angle diffraction patterns characteristic of the lateral packing of the lipids are equivalent in the extracted lipids and the intact SC. This suggests that the second component might form an aggregate containing a significant number of lipids so that the alkyl chains retain their characteristic lateral spacings. The natural tendency is to assume that the second component is a protein. If it is a protein, then it must be a very stable one to resist denaturation for prolonged periods at 70 °C.

It is reasonable to assume that the unit cell of the intercellular domain has a bilayer-type configuration. However, because of the large characteristic repeat distance, the unit cell seems unlikely to be a simple lipid bilayer. Some possibilities include two apposed asymmetric bilayers, symmetric bilayers with asymmetrically distributed protein, or a combination of the two. A reasonable first hypothesis is that the unit cell contains two apposed asymmetric bilayer/protein membranes in the manner of myelin (Schmitt et al., 1941; Worthington, 1969). Freeze–fracture studies (Landmann, 1986) of the so-called membrane coating granules (MCG), which are precursors of the intercellular lamellae, and transmission EM studies of the intercellular lamellae themselves (Madison et al., 1987) reveal structures with alternating densities and/or widths. Both Landmann (1986) and Madison et al. (1987) suggest that the bilayers of the lamellae have asymmetrically distributed lipids. Madison et al. (1987) find a 128-Å repeat period for the intercellular lamellae (in excellent agreement with our value of 131 Å) which is much greater than the values of 96–97 Å observed for MCG (Landmann, 1986; Madison et al., 1987). This suggests to us that an additional component, presumably a protein, enters the intercellular lamellae during the conversion of the MCG. We thus assume, as a working hypothesis, that the intercellular domains contain bilayer/protein complexes and that the unit cell consists of two bilayers and associated proteins.

The relative intensities of the diffraction peaks from the intercellular domains (Figure 2a) give some clues about the structure of the unit cell. If the structure were closely analogous to that of myelin, one would expect alternating weak (odd h) and strong (even h) intensities (Worthington &

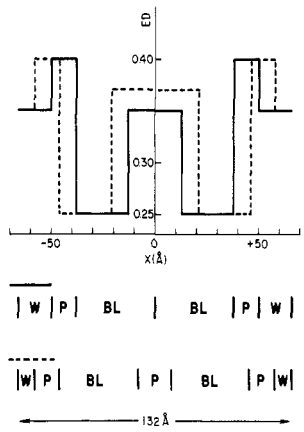

FIGURE 6: Strip-model electron density profiles for two possible models for the unit cell of the intercellular lipid domains. The units of electron density (ED) are electrons per cubic angstrom. The contents of the model unit cells are shown in the bottom half of the figure (BL, bilayer; P, protein; W, water). These models are purely hypothetical and are presented only to show how the symmetry of the two membranes comprising a unit cell can affect the relative intensities of the lines of the diffraction pattern. The solid curve represents the profile of a unit cell with highly asymmetric membranes whereas the dashed curve represents the case of nearly symmetric membranes. The observed relative intensities more nearly match the highly asymmetric case (see text). Proteins on the bilayer surface have only been used to generate the asymmetry for the calculations. The exact nature of the asymmetry is unknown (see text).

Blaurock, 1969). The itensities of Figure 2a do not conform to this pattern; $h = 2$ and 3 are strong, and $h = 4$ and 5 are weak. The limited number of measurements made with double-mirror optics indicate that the first- and second-order peaks have intensities that are well within a factor of 5 of one another. Simple strip-model calculations similar to those of Worthington and Blaurock (1969) suggest that the alternating intensities arise whenever the membranes of the unit cell have a *nearly* symmetric electron density. If, however, the membranes of the unit cell are highly asymmetric, the alternating intensity pattern no longer prevails. As an example of such a calculation, we present in Figure 6 strip-model electron density profiles representing two hypothetical unit cells, each containing a pair of bilayers. In one case (solid curve, Figure 6), each bilayer is coated on only one side with protein so that each membrane of the unit cell is highly asymmetric. In the other case (dashed curve, Figure 6), the bilayers are coated on both sides to make the membranes of the unit cell more symmetric. This nearly symmetric situation yields relative intensities for the $h = 1$–5 diffraction peaks of 0.01, 20.67, 0.08, 6.01, and 0.47, respectively, demonstrating the expected alternating intensity pattern. The highly asymmetric situation, on the other hand, yields relative intensities of 5.01, 5.66, 11.98, 0.48, and 0.47 for $h = 1$–5, respectively. This pattern is more consistent with the observed intensities. Such model-building procedures are not reliable without good information on the intensities and phases of all the peaks and particularly the first-order peak. However, the models do support the general idea that the membranes of the unit cell are likely to be highly asymmetric. There is no evidence to suggest that the supposed protein component is located solely at the bilayer surfaces. This assumption was made purely as a mechanism for introducing a strong asymmetry. Asymmetries could come from various combinations of asymmetric lipid distributions, proteins at the bilayer interface, and bilayer-spanning proteins.

The diffraction pattern observed in SC couplets appears to be a mixture of discrete and continuous diffraction originating from a structure with a characteristic dimension of about 126 Å. It is the type of pattern that might be observed if the multilamellar domains were disrupted so that the diffraction originated from unit cells which were no longer located in a well-ordered lattice. The passage of SC fragments through the cell disrupter at 20 000 psi to produce the couplets has probably had exactly this effect on the intercellular domains. The fact that the apparent unit cell dimension remains largely unchanged after this drastic treatment suggests that the structural entity responsible for the unit cell of the intercellular domain is very durable. Diffraction patterns from completely disaggregated unit cells would be of great value in the determination of the structure of the intercellular domains because such diffraction patterns can, in principle, be deconvoluted uniquely to obtain the electron density profile of the unit cell (Hosemann & Bagchi, 1962; Lesslauer & Blasie, 1972).

Diffraction from Keratin. We expected when we began this work that the keratin of the corneocytes would be clearly visible in the diffraction patterns (Swanbeck, 1959; Swanbeck & Thyresson, 1961, 1962; Goldsmith & Baden, 1970; Wilkes et al., 1973). This turned out not to be the case for the tissue samples we examined. The keratin of skin is generally of the poorly ordered "soft" variety which has an irregular secondary (α) structure which results in a diffraction pattern of two very *diffuse* rings at 4.5 and 9.5 Å (Fraser & MacRae, 1973). We noted earlier (see Results) that two *sharp* lines are seen in SC corresponding to spacings of 4.6 and 9.4 Å (Figure 3). Our first thought was that these must come from keratin that was particularly well-ordered. This possibility was eliminated when we discovered that the pattern persisted unattenuated in the SC couplets which are completely free of keratin (Figure 5). Further, even in the most highly ordered so-called hard keratins (e.g., feathers), the peaks in the vicinity of 4–5 and 9–10 Å are still rather diffuse. The keratin of the hairless mouse skin may be particularly disordered and difficult to observe. In addition, its diffraction pattern may be obscured by the background scatter from the sample at small angles and the liquid alkyl chain diffraction at high angles.

Structure of the Corneocyte Envelopes. Because the lines observed at 4.6 and 9.4 Å in the intact SC are unaffected by temperature and persist in the lipid-extracted keratin-free couplets, they must originate from the corneocyte envelopes or possibly the putative protein component of the intercellular domains. In the lipid-extracted couplets, a weak but sharp third line becomes visible at 3.9 Å (faintly seen in Figure 5 and clearly seen on the original films). The sharpness of the lines is particularly significant; it means that there must be a large regular lattice of unit cells. As we discuss later, one needs about 10 unit cells in a well-ordered lattice to have lines as sharp as these. Taking 10 Å as a characteristic repeat, this means that the structure must be ~100 Å thick. If such a structure were associated with the intercellular domains with alternating layers of lipid (e.g., 60 Å thick), the Bragg spacing would have to be in excess of 300 Å. Further, to account for the sharpness of the small-angle lamellar pattern, one would have to have many layers of these units. The various electron microscopic studies show no evidence of massive amounts of material other than lipid in the intercellular spaces (Elias & Friend, 1975; Lavker, 1976; Elias et al., 1977; Hayward, 1978; Landmann, 1980, 1986; Madison et al., 1987). The corneocyte envelopes are about the only thing seen in lipid-extracted couplets. The possibility of the triad of sharp lines originating from any structure other than the corneocyte envelopes seems very remote.

The corneocyte's protein envelope is known to originate from soluble precursor proteins (M_r 36 000–92 000 depending on species etc.) which become highly cross-linked by transglut-

aminases to produce ε-(γ-glutamyl)lysine bonds (Green, 1980; Goldsmith, 1983; Peterson et al., 1983). The resulting insoluble envelope, which appears to be about 120 Å thick in the electron microscope (Farbman, 1966), is extraordinarily tough and resists completely treatment with subtilisin (Grayson & Elias, 1982) or concentrated NaOH (Maltoltsy & Maltoltsy, 1966).

We were struck by the similarity of our envelope diffraction pattern (Figure 5b) to those observed by Keith et al. (1969) for crystals of β-polyglutamate salts (Ca, Sr, Ba) and acid-precipitated β-polyglutamate. Those crystal structures consist of layers of hydrogen-bonded "sheets" of antiparallel extended polypeptide chains. The crystal lattices have monoclinic unit cells specified by four cell parameters characterizing, basically, the side–side repeat distance of the chains (a), the repeat distance along the chain axes (b), the interlayer spacing (c), and the angle (β) between a and c. The lattice spacings, $d(hkl)$, of the strongest lines observed in wet acid-precipitated β-polyglutamate are 8.8 Å [$d(001)$], 4.7 Å [$d(200)$], and 3.9 Å [$d(210)$] which are surprisingly, and perhaps fortuitously, close to the spacings we observe (9.4, 4.6, and 3.9 Å). If the envelopes have a monoclinic unit cell and if the lines we observe correspond to the same Miller indices, then our data can be satisfactorily indexed with a = 9.4 Å, b = 7.2 Å, c = 9.7 Å, and β = 103.5°. The number of such unit cells [thickness = $d(001)$] spanning the thickness of the envelope (~100 Å) would be 10–12 which should be sufficient to produce sharp discrete diffraction lines (Hosemann & Bagchi, 1962; Lesslauer & Blasie, 1972; Franks & Levine, 1981; Blaurock, 1982).

Involucrin (Green, 1980), the major cytosolic precursor protein for the envelopes of cultured human keratinocytes (corneocytes), has been sequenced by Eckert and Green (1986) using gene cloning methods. The central region of the protein contains 39 repeats of 10 amino acids with each repeat containing 3 glutamines and 2 glutamic acids which are highly conserved throughout the region. A regularly recurring amino acid sequence is gln-glu-glu-gln-gly-gln-leu which is perfectly consistent with our structural hypothesis except for the fact that such a sequence prefers an α-helical conformation by Chou–Fasman (1974) rules ($\langle P_\alpha \rangle$ = 1.21; $\langle P_\beta \rangle$ = 0.89). However, extensive cross-linking of the protein in the envelope is likely to invalidate these rules. It is not unreasonable to think that soluble protein in solution would be α-helical prior to cross-linking into β-pleated sheets by transglutaminase. It is significant that α-helical polyglutamate gels transform into β-pleated sheets at temperatures above 40 °C (Itoh et al., 1976) and that the cross-linking of involucrin occurs only in the presence of calcium (Green, 1980; Goldsmith, 1983; Peterson et al., 1983). The calcium salt of polyglutamate forms β-pleated sheets (Keith et al., 1969).

Swartzendruber et al. (1987) have recently presented evidence suggesting that the plasma membrane of porcine corneocytes is covalently linked through ester linkages of ω-hydroxysphingosines to glutamate residues of the envelope. They propose that the protein assumes β-pleated sheet conformations in the regions of these ester linkages and suggest that such linkages would in fact favor the β conformation through the blockage of the charges of the glutamate residues.

We hypothesize that the basic structural motif of the corneocyte envelopes is highly cross-linked β-sheets but we caution that the hypothesis is speculative. As far as we can establish, no precursor proteins from any species other than human have been sequenced, and the precursors of mouse corneocytes have not been isolated. While it is reasonable to assume that the structural motif of involucrin will prevail in mice and other mammals, this remains a matter of conjecture. Neither involucrin, nor its mRNA, nor its gene has been found in any subprimate (H. Green, personal communication). It should also be noted that there are at least six proteins found in human keratinocytes and/or fibroblasts which can be cross-linked by transglutaminase (Simon & Green, 1984). All of these are noncytosolic proteins, and only two are specific to keratinocytes.

Summary

The data presented in this paper demonstrate that excellent diffraction patterns can be obtained from the lamellar intercellular lipid domains of intact stratum corneum. It is very unlikely that lipid is the sole component of the domains because of the differences between the small-angle diffraction patterns from the domains and from the extracted lipids. We hypothesize, but have not proven, that a protein component exists in the intercellular domains which creates a basic structural unit consisting of two bilayers with highly asymmetrically distributed protein. We have also demonstrated that diffraction patterns can be obtained from the corneocyte envelopes. We hypothesize, but have not proven, that the protein of the envelope consists of highly cross-linked β-sheets.

Acknowledgments

We thank Allergan, Inc., for a gift which made this work possible. We appreciate the encouragement of Dr. Peter Elias and his group and particularly the help of Dr. Stephen Grayson, who isolated the couplets used in this study, and the invaluable comments of Drs. Robert McDaniel and Donald Engelman on early versions of the manuscript.

References

Blank, I. H. (1952) *J. Invest. Dermatol. 18*, 433–440.
Blaurock, A. E. (1982) *Biochim. Biophys. Acta 650*, 167–207.
Bligh, E. G., & Dyer, W. J. (1959) *Can. J. Biochem. Physiol. 37*, 911–917.
Bowser, P. A., & White, R. J. (1985) *Br. J. Dermatol. 112*, 1–14.
Brody, I. (1959) *J. Ultrastruct. Res. 2*, 482–511.
Chou, P. Y., & Fasman, G. D. (1974) *Biochemistry 13*, 222–244.
Eckert, R. L., & Green, H. (1986) *Cell (Cambridge, Mass.) 46*, 583–589.
Elias, P. M. (1983) *J. Invest. Dermatol. 80*, 44s–49s.
Elias, P. M., & Friend, D. S. (1975) *J. Cell Biol. 65*, 185–191.
Elias, P. M., Goerke, J., & Friend, D. S. (1977) *J. Invest. Dermatol. 69*, 535–546.
Elias, P. M., Brown, B. E., Fritsch, P., Goerke, J., Gray, G. M., & White, R. J. (1979) *J. Invest. Dermatol. 73*, 339–348.
Elias, P. M., Cooper, E. R., Korc, A., & Brown, B. E. (1981) *J. Invest. Dermatol. 76*, 297–301.
Elias, P. M., Bonar, L., Grayson, S., & Baden, H. (1983) *J. Invest. Dermatol. 80*, 213–214.
Elliott, A. (1965) *J. Sci. Instrum. 42*, 312–316.
Farbman, A. I. (1966) *Anat. Rec. 156*, 269–282.
Franks, A. (1958) *Br. J. Appl. Phys. 9*, 349–352.
Franks, N. P., & Levine, Y. K. (1981) in *Membrane Spectroscopy* (Grell, E., Ed.) pp 437–487, Springer-Verlag, Berlin.
Fraser, R. D. B., & MacRae, T. P. (1973) *Conformation in Fibrous Proteins*, Academic, New York.
Friberg, S. E., Osborne, D. W., & Tombridge, T. L. (1985) *J. Soc. Cosmet. Chem. 36*, 349–354.

Golden, G. M., Guzek, D. B., Kennedy, A. E., McKie, J. E., & Potts, R. O. (1987) *Biochemistry 26*, 2382–2388.
Goldsmith, L. A. (1983) *J. Invest. Dermatol. 80*, 39–41.
Goldsmith, L. A., & Baden, H. P. (1970) *Nature (London) 225*, 1052–1053.
Gray, G. M., & Yardley, H. J. (1975) *J. Lipid Res. 16*, 441–447.
Grayson, S., & Elias, P. M. (1982) *J. Invest. Dermatol. 78*, 128–135.
Green, H. (1980) *Harvey Lect. 74*, 101–139.
Hayward, A. F. (1978) *Cell Tissue Res. 187*, 323–331.
Hosemann, R., & Bagchi, S. N. (1962) *Direct Analysis of Diffraction by Matter*, North-Holland, Amsterdam.
Itoh, K., Foxman, B. M., & Fasman, G. D. (1976) *Biopolymers 15*, 419–455.
Janiak, M. J., Small, D. M., & Shipley, G. G. (1979) *J. Biol. Chem. 254*, 6068–6078.
Keith, H. D., Padden, F. J., & Giannoni, G. (1969) *J. Mol. Biol. 43*, 423–438.
King, G. I., & White, S. H., (1986) *Biophys. J. 49*, 1047–1054.
Knutson, K., Potts, R. O., Guzek, D. B., Golden, G. M., McKie, J. E., Lambert, W. J., & Higuchi, W. I. (1985) *J. Controlled Release 2*, 67–87.
Lampe, M. A., Williams, M. L., & Elias, P. M. (1983) *J. Lipid Res. 24*, 131–140.
Landmann, L. (1980) *J. Ultrastruct. Res. 72*, 245–263.
Landmann, L. (1986) *J. Invest. Dermatol. 87*, 202–209.
Lavker, R. S. (1976) *J. Ultrastruct. Res. 55*, 79–86.
Lesslauer, W., & Blasie, J. K. (1972) *Biophys. J. 12*, 175–190.
Madison, K. C., Swartzendruber, D. C., Wertz, P. W., & Downing, D. T. (1987) *J. Invest. Dermatol. 88*, 714–718.
Maltoltsy, A. G., & Maltoltsy, M. S. (1966) *J. Invest. Dermatol. 46*, 127–129.
Marks, R., & Plewig, G., Eds. (1986) *Stratum Corneum*, Springer-Verlag, Berlin.
Mirejovsky, D., & Takruri, H. (1986) *J. Pharm. Sci. 75*, 1089–1093.
Peterson, L. L., Zettergren, J. G., & Wuepper, K. D. (1983) *J. Invest. Dermatol. 81*, 95s–100s.
Ranck, J. L., Mateu, L., Sadler, D. M., Tardieu, A., Gulik-Krzywicki, T., & Luzzati, V. (1974) *J. Mol. Biol. 85*, 249–277.
Rehfeld, S. J., & Elias, P. M. (1982) *J. Invest. Dermatol. 79*, 1–3.
Schaefer, H., Zesch, A., & Stüttgen, G., Eds. (1982) *Skin Permeability*, Springer-Verlag, Berlin.
Schmitt, F. O., Bear, R. S., & Palmer, K. J. (1941) *J. Cell. Comp. Physiol. 18*, 31–42.
Simon, M., & Green, H. (1984) *Cell (Cambridge, Mass.) 36*, 827–834.
Small, D. M. (1986) *The Physical Chemistry of Lipids*, Plenum, New York.
Smith, W. P., Christensen, M. S., Nacht, S., & Gans, E. H. (1982) *J. Invest. Dermatol. 78*, 7–11.
Swanbeck, G. (1959) *Acta Derm.-Venereol. 39 (Suppl. 43)*, 5–37.
Swanbeck, G., & Thyresson, N. (1961) *Acta Derm.-Venereol. 41*, 289–296.
Swanbeck, G., & Thyresson, N. (1962) *Acta Derm.-Venereol. 42*, 445–457.
Swartzendruber, D. C., Wertz, P. W., Madison, K. C., & Downing, D. T. (1987) *J. Invest. Dermatol. 88*, 709–713.
Wilkes, G. L., Nguyen, A.-L., & Wildnauer, R. (1973) *Biochim. Biophys. Acta 304*, 267–275.
Woodford, R., & Barry, B. W. (1986) *J. Toxicol., Cutaneous Ocul. Toxicol. 5*, 167–177.
Worthington, C. R. (1969) *Proc. Natl. Acad. Sci. U.S.A. 63*, 604–611.
Worthington, C. R., & Blaurock, A. E. (1969) *Biophys. J. 9*, 970–990.